Power optimization of XUV frequency combs for spectroscopy applications [Invited]

D. C. Yost,[1,*] A. Cingöz,[1] T. K. Allison,[1] A. Ruehl,[2,3] M. E. Fermann,[2] I. Hartl,[2] and J. Ye[1]

[1]*JILA, National Institute of Standards and Technology, and University of Colorado Department of Physics, University of Colorado, Boulder, Colorado 80309-0440, USA*

[2]*IMRA America, Inc., 1044 Woodridge Avenue, Ann Arbor, Michigan 48105, USA*

[3]*Present address: Institute for Lasers, Life and Biophotonics, Vrije Universiteit Amsterdam, De Boelelaan 1081, 1081HV Amsterdam, The Netherlands*

[*]*dylan.yost@colorado.edu*

Abstract: We address technical impediments to the generation of high-photon flux XUV frequency combs through cavity-enhanced high harmonic generation. These difficulties arise from mirror damage, cavity nonlinearity, the intracavity plasma generated during the HHG process, and imperfect phase-matching. By eliminating or minimizing each of these effects we have developed a system capable of generating > 200 μW and delivering ~20 μW of average power for each spectrally separated harmonic (wavelengths ranging from 50 nm - 120 nm), to actual comb-based spectroscopy experiments.

OCIS codes: (190.7110) Ultrafast nonlinear optics; (300.6540) Spectroscopy, ultraviolet.

References and links

1. T. K. Allison, T. W. Wright, A. M. Stooke, C. Khurmi, J. van Tilborg, Y. Liu, R. W. Falcone, and A. Belkacem, "Femtosecond spectroscopy with vacuum ultraviolet pulse pairs," Opt. Lett. **35**(21), 3664–3666 (2010).
2. A. Ravasio, D. Gauthier, F. R. N. C. Maia, M. Billon, J.-P. Caumes, D. Garzella, M. Géléoc, O. Gobert, J. F. Hergott, A. M. Pena, H. Perez, B. Carré, E. Bourhis, J. Gierak, A. Madouri, D. Mailly, B. Schiedt, M. Fajardo, J. Gautier, P. Zeitoun, P. H. Bucksbaum, J. Hajdu, and H. Merdji, "Single-shot diffractive imaging with a table-top femtosecond soft x-ray laser-harmonics source," Phys. Rev. Lett. **103**(2), 028104 (2009).
3. Z. H. Loh and S. R. Leone, "Ultrafast strong-field dissociative ionization dynamics of CH_2Br_2 probed by femtosecond soft x-ray transient absorption spectroscopy," J. Chem. Phys. **128**(20), 204302 (2008).
4. F. Krausz and M. Ivanov, "Attosecond physics," Rev. Mod. Phys. **81**(1), 163–234 (2009).
5. D. Z. Kandula, Ch. Gohle, T. J. Pinkert, W. Ubachs, and K. S. E. Eikema, "Extreme ultraviolet frequency comb metrology," Phys. Rev. Lett. **105**(6), 063001 (2010).
6. R. J. Jones, K. D. Moll, M. J. Thorpe, and J. Ye, "Phase-coherent frequency combs in the vacuum ultraviolet via high-harmonic generation inside a femtosecond enhancement cavity," Phys. Rev. Lett. **94**(19), 193201 (2005).
7. Ch. Gohle, Th. Udem, M. Herrmann, J. Rauschenberger, R. Holzwarth, H. A. Schuessler, F. Krausz, and T. W. Hänsch, "A frequency comb in the extreme ultraviolet," Nature **436**(7048), 234–237 (2005).
8. A. Marian, M. C. Stowe, J. R. Lawall, D. Felinto, and J. Ye, "United time-frequency spectroscopy for dynamics and global structure," Science **306**(5704), 2063–2068 (2004).
9. A. Marian, M. C. Stowe, D. Felinto, and J. Ye, "Direct frequency comb measurements of absolute optical frequencies and population transfer dynamics," Phys. Rev. Lett. **95**(2), 023001 (2005).
10. E. E. Eyler, D. E. Chieda, M. C. Stowe, M. J. Thorpe, T. R. Schibli, and J. Ye, "Prospects for precision measurements of atomic helium using direct frequency comb spectroscopy," Eur. Phys. J. D **48**(1), 43–55 (2008).
11. M. Herrmann, M. Haas, U. D. Jentschura, F. Kottmann, D. Leibfried, G. Saathoff, Ch. Gohle, A. Ozawa, V. Batteiger, S. Knünz, N. Kolachevsky, H. A. Schüssler, T. W. Hänsch, and Th. Udem, "Feasibility of coherent xuv spectroscopy on the 1*S*-2*S* transition in singly ionized helium," Phys. Rev. A **79**(5), 052505 (2009).
12. J. Lee, D. R. Carlson, and R. J. Jones, "Optimizing intracavity high harmonic generation for XUV fs frequency combs," Opt. Express **19**(23), 23315–23326 (2011).
13. T. Eidam, S. Hanf, E. Seise, T. V. Andersen, T. Gabler, C. Wirth, T. Schreiber, J. Limpert, and A. Tünnermann, "Femtosecond fiber CPA system emitting 830 W average output power," Opt. Lett. **35**(2), 94–96 (2010).
14. A. Vernaleken, J. Weitenberg, T. Sartorius, P. Russbueldt, W. Schneider, S. L. Stebbings, M. F. Kling, P. Hommelhoff, H. D. Hoffmann, R. Poprawe, F. Krausz, T. W. Hänsch, and T. Udem, "Single-pass high-harmonic generation at 20.8 MHz repetition rate," Opt. Lett. **36**(17), 3428–3430 (2011).

#154969 - $15.00 USD Received 19 Sep 2011; revised 26 Oct 2011; accepted 27 Oct 2011; published 2 Nov 2011

15. C. J. Saraceno, O. H. Heckl, C. R. Baer, T. Südmeyer, and U. Keller, "Pulse compression of a high-power thin disk laser using rod-type fiber amplifiers," Opt. Express **19**(2), 1395–1407 (2011).
16. A. Ruehl, A. Marcinkevicius, M. E. Fermann, and I. Hartl, "80 W, 120 fs Yb-fiber frequency comb," Opt. Lett. **35**(18), 3015–3017 (2010).
17. I. Hartl, G. Imeshev, L. Dong, G. C. Cho, and M. E. Fermann, "Ultra-compact dispersion compensated femtosecond fiber oscillators and amplifiers," in Conference on Lasers and Electro-Optics/Quantum Electronics and Laser Science and Photonic Applications Systems Technologies, Technical Digest (CD) (Optical Society of America, 2005), paper CThG1. *http://www.opticsinfobase.org/abstract.cfm?URI=CLEO-2005-CThG1*
18. S. Ramachandran, S. Ghalmi, J. W. Nicholson, M. F. Yan, P. Wisk, E. Monberg, and F. V. Dimarcello, "Anomalous dispersion in a solid, silica-based fiber," Opt. Lett. **31**(17), 2532–2534 (2006).
19. M. E. Fermann, M. L. Stock, A. Galvanauskas, G. C. Cho, and B. C. Thomsen, "Third-order dispersion control in ultrafast Yb fiber amplifiers", Conf. on Advanced Solid State Lasers, ASSL 2001, paper TuA3.
20. K. Moll, R. Jones, and J. Ye, "Nonlinear dynamics inside femtosecond enhancement cavities," Opt. Express **13**(5), 1672–1678 (2005).
21. D. C. Yost, T. R. Schibli, and J. Ye, "Efficient output coupling of intracavity high-harmonic generation," Opt. Lett. **33**(10), 1099–1101 (2008).
22. I. Pupeza, T. Eidam, J. Rauschenberger, B. Bernhardt, A. Ozawa, E. Fill, A. Apolonski, Th. Udem, J. Limpert, Z. A. Alahmed, A. M. Azzeer, A. Tünnermann, T. W. Hänsch, and F. Krausz, "Power scaling of a high-repetition-rate enhancement cavity," Opt. Lett. **35**(12), 2052–2054 (2010).
23. Y.-Y. Yang, F. Süßmann, S. Zherebtsov, I. Pupeza, J. Kaster, D. Lehr, H.-J. Fuchs, E.-B. Kley, E. Fill, X.-M. Duan, Z.-S. Zhao, F. Krausz, S. L. Stebbings, and M. F. Kling, "Optimization and characterization of a highly-efficient diffraction nanograting for MHz XUV pulses," Opt. Express **19**(3), 1954–1962 (2011).
24. K. D. Moll, R. J. Jones, and J. Ye, "Output coupling methods for cavity-based high-harmonic generation," Opt. Express **14**(18), 8189–8197 (2006).
25. A. Ozawa, A. Vernaleken, W. Schneider, I. Gotlibovych, Th. Udem, and T. W. Hänsch, "Non-collinear high harmonic generation: a promising outcoupling method for cavity-assisted XUV generation," Opt. Express **16**(9), 6233–6239 (2008).
26. J. Weitenberg, P. Rußbüldt, T. Eidam, and I. Pupeza, "Transverse mode tailoring in a quasi-imaging high-finesse femtosecond enhancement cavity," Opt. Express **19**(10), 9551–9561 (2011).
27. I. Pupeza, E. E. Fill, and F. Krausz, "Low-loss VIS/IR-XUV beam splitter for high-power applications," Opt. Express **19**(13), 12108–12118 (2011).
28. T. Tamir and S. T. Peng, "Analysis and design of grating couplers," Appl. Phys. (Berl.) **14**(3), 235–254 (1977).
29. E. Constant, D. Garzella, P. Breger, E. Mével, Ch. Dorrer, C. Le Blanc, F. Salin, and P. Agostini, "Optimizing high harmonic generation in absorbing gases: model and experiment," Phys. Rev. Lett. **82**(8), 1668–1671 (1999).
30. T. K. Allison, A. Cingöz, D. C. Yost, and J. Ye, "Extreme nonlinear optics in a femtosecond enhancement cavity," Phys. Rev Lett. **107**, 183903 (2011).
31. D. R. Carlson, J. Lee, J. Mongelli, E. M. Wright, and R. J. Jones, "Intracavity ionization and pulse formation in femtosecond enhancement cavities," Opt. Lett. **36**(15), 2991–2993 (2011).
32. E. P. Kanter, R. Santra, C. Höhr, E. R. Peterson, J. Rudati, D. A. Arms, E. M. Dufresne, R. W. Dunford, D. L. Ederer, B. Krässig, E. C. Landahl, S. H. Southworth, and L. Young, "Characterization of the spatiotemporal evolution of laser-generated plasmas," J. Appl. Phys. **104**(7), 073307 (2008).
33. R. W. Boyd, *Nonlinear Optics*, Second Edition (Academic, 2003).
34. A. Cingöz, D. C. Yost, T. K. Allison, A. Ruehl, M. E. Fermann, I. Hartl, and J. Ye, "Broadband phase noise suppression in a Yb-fiber frequency comb," Opt. Lett. **36**(5), 743–745 (2011).
35. I. Hartl, T. R. Schibli, A. Marcinkevicius, D. C. Yost, D. D. Hudson, M. E. Fermann, and J. Ye, "Cavity-enhanced similariton Yb-fiber laser frequency comb: 3 x 10^{14} W/ cm^2 peak intensity at 136 MHz," Opt. Lett. **32**(19), 2870–2872 (2007).
36. T. R. Schibli, I. Hartl, D. C. Yost, M. J. Martin, A. Marcinkevičius, M. E. Fermann, and J. Ye, "Optical frequency comb with submillihertz linewidth and more than 10 W average power," Nat. Photonics **2**(6), 355–359 (2008).
37. A. Ozawa, J. Rauschenberger, Ch. Gohle, M. Herrmann, D. R. Walker, V. Pervak, A. Fernandez, R. Graf, A. Apolonski, R. Holzwarth, F. Krausz, T. W. Hänsch, and Th. Udem, "High harmonic frequency combs for high resolution spectroscopy," Phys. Rev. Lett. **100**(25), 253901 (2008).
38. D. C. Yost, T. R. Schibli, J. Ye, J. L. Tate, J. Hostetter, M. B. Gaarde, and K. J. Schafer, "Vacuumultraviolet frequency combs from below-threshold harmonics," Nat. Phys. **5**, 815 (2009).
39. A. Cingöz, D. C. Yost, T. K. Allison, A. Ruehl, M. E. Fermann, I. Hartl, and J. Ye, "Direct frequency comb spectroscopy in the extreme ultraviolet," Accepted to Nature (2011).
40. J. Tate, T. Auguste, H. G. Muller, P. Salières, P. Agostini, and L. F. DiMauro, "Scaling of wave-packet dynamics in an intense midinfrared field," Phys. Rev. Lett. **98**(1), 013901 (2007).
41. L. D. Merkle, N. Koumvakalis, and M. Bass, "Laser-induced bulk damage in SiO2 at 1.064, 0.532, and 0.355 µm," J. Appl. Phys. **55**(3), 772 (1984).
42. I. J. Kim, G. H. Lee, S. B. Park, Y. S. Lee, T. K. Kim, C. H. Nam, T. Mocek, and K. Jakubczak, "Generation of submicrojoule high harmonics using a long gas jet in a two-color laser field," Appl. Phys. Lett. **92**(2), 021125 (2008).

#154969 - $15.00 USD Received 19 Sep 2011; revised 26 Oct 2011; accepted 27 Oct 2011; published 2 Nov 2011

43. E. Takahashi, Y. Nabekawa, and K. Midorikawa, "Generation of 10- μJ coherent extreme-ultraviolet light by use of high-order harmonics," Opt. Lett. **27**(21), 1920–1922 (2002).
44. J.-F. Hergott, M. Kovacev, H. Merdji, C. Hubert, Y. Mairesse, E. Jean, P. Breger, P. Agostini, B. Carré, and P. Salières, "Extreme-ultraviolet high-order harmonic pulses in the microjoule range," Phys. Rev. A **66**(2), 021801 (2002).
45. S. Hädrich, J. Rothhardt, M. Krebs, F. Tavella, A. Willner, J. Limpert, and A. Tünnermann, "High harmonic generation by novel fiber amplifier based sources," Opt. Express **18**(19), 20242–20250 (2010).
46. D. Attwood, *Soft X-rays and extreme ultraviolet radiation* (Cambridge University Press, 1999).

1. Introduction

Amplified femtosecond laser systems driving the high harmonic process have become ubiquitous sources of XUV radiation. These table-top, short-wavelength sources have found successful application in experiments ranging from time-resolved attosecond dynamics to lenseless imaging [1–4]. In a different research direction, as a versatile, laser-like source of radiation, HHG sources have stimulated interest in their potential use for high-resolution XUV frequency metrology. However, most routes to high harmonic generation use pulsed lasers with repetition frequencies from 10 Hz to 100 kHz. These sources are typically utilized in single pulse experiments where the IR pulse leads to a single burst of attosecond XUV pulses (the Fourier transform of this single burst of attosecond pulses results in the high harmonic spectrum with multiple harmonic orders). Since only a single harmonic pulse is utilized, this produces an XUV source with a broad bandwidth not suitable for high-resolution spectroscopy. Recent spectroscopy measurements in the XUV have been performed utilizing two-pulse Ramsey spectroscopy in an effort to circumvent this challenge [5]. These measurements, however, require careful calibration of phase shifts in the system, which produce a systematic error. In a frequency comb-based measurement this systematic error is removed, since the comb structure is rigorously defined with a continuous train of high repetition rate pulses.

Much higher repetition rates are obtainable through the femtosecond enhancement cavity (FEC) technique, which has demonstrated the ability to drive the high harmonic process at:100 MHz repetition rates [6,7]. In this approach, a femtosecond laser is used to excite the resonances of a passive optical cavity providing a large augmentation of the intracavity pulse energy that is then used to drive the HHG process at the original repetition frequency of the modelocked laser. The Fourier transform of the electric field of such a continuous source of pulses (if phase coherent) produces a comb of narrow linewidth XUV frequencies- exactly analogous to the visible frequency combs that have been revolutionary for visible high-resolution spectroscopy. These XUV combs provide additional underlying frequency structure within the odd harmonics produced in HHG, leading to spectral resolution in the XUV limited by a single comb tooth. While visible frequency combs are most often utilized as a calibration tool for continuous wave (CW) spectroscopic lasers, it has been shown that the frequency comb can also be used directly as a spectroscopic tool without CW lasers- a technique named direct frequency comb spectroscopy (DFCS) [8]. Since there are currently no CW lasers suitable for high-resolution spectroscopy in the XUV, there is much hope that the combination of DFCS and the XUV frequency comb can help bring ultrahigh resolution laser spectroscopy to spectral regions that have been quite difficult to access previously.

A significant challenge facing high-resolution spectroscopy with an XUV frequency comb is the low average power available through the HHG process. When exciting a one-photon transition in DFCS, the optical power available for spectroscopy is effectively that of a single frequency comb tooth [9]. As an example, a typical frequency comb will likely have ~ 10^4 to 10^6 comb teeth. Therefore, an XUV frequency comb boasting 1 μW of average power may have only 1-100 pW of power available for spectroscopy. When exciting a 2-photon transition the entire power of the frequency comb becomes available for spectroscopy, but transition rates are intrinsically lower so that in both cases the experiments are likely to be photon flux limited [10,11]. This highlights the need to boost the average power of an XUV frequency

#154969 - $15.00 USD Received 19 Sep 2011; revised 26 Oct 2011; accepted 27 Oct 2011; published 2 Nov 2011

comb while maximizing the power delivered to the atoms or molecules to be probed with a carefully designed spectroscopic system. While the average XUV power available from the FEC technique should be high due to the very large circulating average power at the fundamental wavelength (~10 kW), difficulties intrinsic to the enhancement cavity have presented challenges to surpassing the average XUV flux demonstrated by single pass systems (systems that do not utilize a FEC). Here we outline some of the most prominent difficulties and demonstrate a system which mitigates or overcomes many of these issues, providing a high brightness XUV source capable of delivering a large fraction of the generated power directly to spectroscopic experiments.

2. Challenges intrinsic to the driving frequency comb, cavity optics and output coupling techniques

The very large peak intracavity power required to drive the HHG process can present challenges to generating a useable XUV frequency comb. First, a high average power femtosecond frequency comb laser is required to excite the enhancement cavity. While power-scaling femtosecond Ti:Sapp lasers at a fundamental repetition frequency of 50 MHz to the 7-W level has been demonstrated [12], the lack of efficient high-power CW pump sources prevents significantly higher powers. Direct diode pumped Yb-solid state and Yb-fiber laser technology allows scaling the average power of ultrafast laser systems towards the kW-level [13,14]. However, for low-noise optical phase control and efficient HHG clean ultra-short pulses are required, a specification difficult to fulfill both in Yb:YAG and Yb-fiber systems. Yb:YAG lasers are gain-bandwidth limited to ~700 fs. The generation of shorter pulses is possible using nonlinear broadening and re-compression which limits the output power at a much lower level due to material damage in the spectral broadening stage [14,15]. In Yb:fiber systems power scaling without non-linear pulse-distortion requires chirped pulse amplification with large stretching ratios, where a large dispersion needs to be perfectly balanced in order to achieve Fourier-limited pulses.

For the studies presented here, we excite the optical enhancement cavity with an 80-W Yb-fiber frequency comb, the highest average power frequency comb demonstrated to date. The system, described in detail in [16], is based on a Fabry-Perot type Yb-fiber similariton oscillator mode-locked with a sub-ps lifetime saturable absorber [17]. It produces a 154 MHz pulse train with excellent passive phase noise properties reflected by the free-running carrier-envelope offset beat linewidth of less than 15 kHz. For coherent phase locking, we implemented a slow and a fast feedback loop for each comb parameter. Pulse stretching was realized with a total length of > 380 m passive fiber. The fiber stretcher was concatenated from three different sections of fiber of widely differing dispersion characteristics, which included higher order mode (HOM) fiber [18], anomalous third-order dispersion fiber [19] and regular single-mode fiber. Appropriate selection of the compressor grating groove density and incidence angle (selected here for a Littrow configuration) thus allowed matching the overall dispersion of the system to quartic order. We used three Yb-fiber based, saturated amplifier stages of 15 dB gain each at a wavelength of 1070 nm, representing a good compromise between amplifier bandwidth and gain per unit length. The final amplifier, seeded with 3.4 W, consisted of 9 m polarization maintaining double-clad large mode area Yb-fiber with an effective core area of 600 μm^2, end-pumped by 915 nm diode bars.

The pulses amplified to 108 W had 20 nm FWHM bandwidth centered at 1070 nm and durations of 370 ps. Using a polymer transmission grating compressor with 1590 lines / mm operated at Littrow-angle, the pulses were re-compressed to 120 fs with less than 14% of the pulse energy in the remaining pedestal. Due to the compressor efficiency of 74%, the average power of the compressed pulses was 80 W, corresponding to 0.52 μJ pulse energy.

At an average power of 30 W from the driving frequency comb, we achieve > 7 kW of average intracavity power and 380 MW of peak power. Under these conditions, the optical elements comprising the cavity can become damaged or present a nonlinear response that

#154969 - $15.00 USD Received 19 Sep 2011; revised 26 Oct 2011; accepted 27 Oct 2011; published 2 Nov 2011

complicates the cavity-comb coupling. While in a single-pass HHG system small nonlinearities usually go unnoticed, within the cavity the nonlinearity can dramatically impede the optical coupling efficiency [20]. Our cavity, including the XUV output coupler [21], consists exclusively of high reflectivity dielectric mirrors that demonstrate a low level of nonlinearity due to the short interaction depth of the mirror surface. Damage on high-reflectivity cavity mirrors will typically result in increased absorption and thermal stress on the cavity optical elements, ultimately leading to cavity misalignment. We implement mirrors with a high damage threshold attributed to the careful design of coating layer materials and thicknesses. It should be noted that in a femtosecond enhancement cavity without an output coupler or target gas, Pupeza *et al.* have demonstrated 18 kW of average power with 200 fs pulses [22]. Our cavity is limited to ~7 kW of average power due to the presence of the target gas. Without target gas we are able to achieve more than 10 kW of average power, reaching comparable peak powers to [22] considering our shorter pulse duration.

One of the most obvious challenges to the FEC technique, which has generated much interest in the literature, is the need for a robust and effective output coupler for the generated light [21,23–27]. Ideally this optical element or technique should couple the harmonic XUV radiation out of enhancement cavity while leaving the fundamental radiation unaffected. We previously introduced a method whereby we etch a small-period diffraction grating directly into the first layer of a high-reflectance multi-layer dielectric cavity mirror [21]. If the period of this diffraction grating is short enough, the fundamental light will only possess zeroth-order diffraction such that this optic will appear as a high reflector to the fundamental but will serve as a diffraction grating in the XUV. In our case, we use a 420 nm period grating at a 70° angle of incidence. The efficiency of this technique is ~10%. An increase in third harmonic generation (30% with error bars of nearly equal magnitude) was observed from a subwavelength blazed diffraction grating output coupler when compared to a plain dielectric mirror [23]. This effect could, in principle, introduce a slight amount of loss but is insignificant when compared with the losses and nonlinearities introduced from a laser ionized gas target (discussed in the section 3). We emphasize that while at large intracavity power cavity optics can become damaged, the grating output coupler is, in our experience, as robust as any other high reflector in the cavity. We therefore do not anticipate the output coupler to limit cavity operation in any significant way.

Any output coupling technique that sends harmonic and residual fundamental radiation from the cavity collinearly will usually require spectral filtering to select only the desired harmonic for the experiment. The two most common methods to achieve this filtering are through diffraction gratings or thin metallic filters. Without this filtering any spectroscopic experiment must be designed to be impervious to the potentially ionizing radiation of the high harmonics and the AC stark shifts from the lower harmonics and the fundamental radiation. In the XUV, such spectral filtering will typically possess only ~10% - 20% efficiency under good conditions. By combining the spectral filtering element and the output coupler we are thus able to deliver ~10 times more photons to spectroscopy experiments. Additionally, the small-period diffraction grating method produces a TEM_{00} harmonic beam as compared with other output-coupling methods relying on higher-order transverse-mode fundamental beams [24–26]. When doing spectroscopy with relatively low power and using spectroscopic techniques that are susceptible to scattered background radiation, a TEM_{00} harmonic beam provides a major advantage.

The diffraction grating output coupler must be designed carefully to meet several criteria: 1) the diffraction efficiency of the optic should be optimized for XUV wavelengths of interest, 2) the optic should have high reflectivity at the fundamental wavelength, and 3) the optical damage threshold of the optic should be as high as possible. The efficiency of the grating at XUV wavelengths is highest when the period of the grating is as long as possible while still being short enough to have no diffracted orders for the fundamental radiation. The

#154969 - $15.00 USD Received 19 Sep 2011; revised 26 Oct 2011; accepted 27 Oct 2011; published 2 Nov 2011

fundamental radiation incident on a subwavelength diffraction grating will produce an evanescent wave with decay constant, α, given by:

$$\alpha = 2\pi\sqrt{\left(\frac{\sin(\theta)}{\lambda}+\frac{m}{\lambda_g}\right)^2-\frac{n^2}{\lambda^2}}, \quad (1)$$

where λ is the vacuum wavelength of the fundamental radiation, λ_g is the grating period, n is the index of the upper layer of the dielectric stack (in our case SiO_2 with an index of 1.45), θ is the angle of incidence, and m is the order number. Equation (1) is found by matching boundary conditions at the grating surface. When conditions 1 and 2 discussed above are fulfilled, α approaches zero for the $m = -1$ order and the evanescent wave extends deep into the upper layer of the dielectric coating. It is important to take this evanescent wave into consideration when designing a grating output coupler. If the evanescent wave extends to the first high index layer of the dielectric stack (with an index of ~1.9), α will be imaginary in that layer- this corresponds to a traveling wave. Therefore optical power can be coupled to a waveguide comprised of the first high index layer of the mirror dielectric stack sandwiched between low index SiO_2 layers. Through this mechanism, the fundamental radiation incident on the optic can experience additional loss. The waveguide coupling efficiency depends on the precise wavelength and angle of the grating [28]. For our grating parameters α is equal to 0.004 nm^{-1} so that the electric field drops to its 1/*e* value in 250 nm.

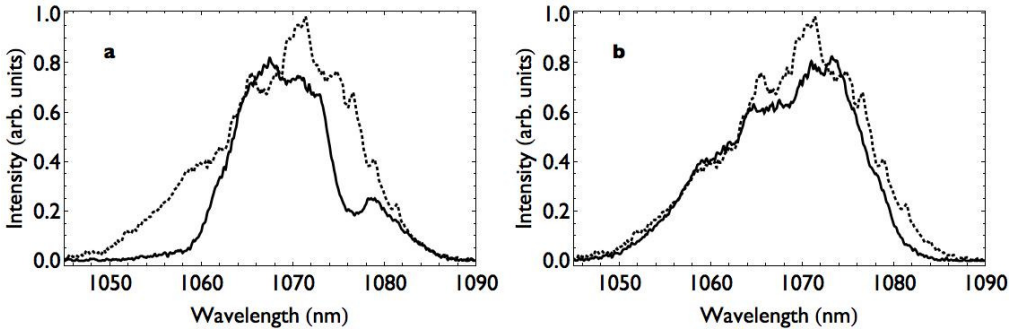

Fig. 1. The laser spectrum incident on the enhancement cavity is compared with the intracavity spectrum for two different designs of grating output coupler. a) solid curve is the intracavity spectrum for grating output coupler with 100 nm SiO_2 top layer. Dotted curve is the incident spectrum for comparison. b) same as in a) but with 460 nm SiO_2 top layer for which the lack of evanescent waveguide coupling is clearly evident. Some difference between the incident and the intracavity spectra is attributed to intracavity mirror dispersion.

In Fig. 1, we compare intracavity spectra for similar grating designs– the first with a 100 nm thick upper SiO_2 layer (0.4 x the 1/*e* decay constant) and the second with a 460 nm upper layer (~2 x the 1/*e* constant). As can be seen from the figure, the thinner SiO_2 upper layer can efficiently couple power into the high index layer producing loss at certain wavelengths. This effect is absent for the thicker upper layer since the power in the evanescent wave has decayed by ~$1/e^4$. In principle, one could also decrease the waveguide coupling efficiency by decreasing the period of the diffraction grating, but this tends to decrease the grating efficiency for the harmonic wavelengths whereas increasing the upper layer thickness has no effect on the grating operation in the XUV.

3. Effect of plasma phase shifts on the enhancement cavity

Significant limitations to FEC operation can originate from the plasma at the intracavity focus intrinsic to the HHG process. In a system optimized for XUV flux, the density length product of the target gas should be increased until the HHG production is in the so-called absorption

#154969 - $15.00 USD Received 19 Sep 2011; revised 26 Oct 2011; accepted 27 Oct 2011; published 2 Nov 2011

limit [29]. If we approach this gas density and ionize a significant fraction of the target gas with every pass of the intracavity pulse, the laser-generated plasma can reach a density such that a significant phase shift of the fundamental occurs. In addition to presenting problems for the phase-matching of HHG, here the phase-shift also affects the cavity performance. We estimate that for the studies presented here, the free electron density can approach $\approx 10^{17}$ cm^{-3}, which over the length of the medium can produce a significant round trip phase shift of ≈0.1 rad. For a high-repetition rate system, the intracavity pulse will interact with a given electron in the plasma several times before the plasma dissipates out of the interaction region. One can, therefore, consider two different contributions to the plasma density which in turn present their own unique challenges; a steady-state density which persists from pulse to pulse and a density that increases rapidly over the duration of the pulse [30,31]. A reasonable rate for plasma dissipation results in a persisting plasma density that is 5 − 10 times higher than the dynamic density [32].

The main consequence of the plasma density that is persisting over the repetition period is to create instability in the frequency lock of the femtosecond laser to the buildup cavity. The intracavity power as a function of detuning from the cavity resonance is illustrated by the blue curve in Fig. 2a. With the addition of target gas, plasma whose density depends nonlinearly on the intracavity power will create a shift in the absolute frequency of the cavity resonance as shown by the dotted green curve in Fig. 2a. This detuning-dependent frequency shift modifies the trivial linear relationship between laser frequency and resonant detuning as shown in Fig. 2b. This is a manifestation of optical bistability as the portion of the curve with the negative slope (the dotted green line in part b) is unstable, which can be confirmed with a linear stability analysis [33].

In a typical frequency lock that aims to minimize the comb detuning from the resonance, the cavity will lock very close to the unstable branch (point 1 in Fig. 2b). Small residual frequency error can push the system to the unstable branch after which the system will jump to point 2 in Fig. 2b. The frequency lock will correct this sudden error moving the system through points 2-4 and eventually arriving back at point 1. As this process repeats, oscillations in the system will occur. The system becomes more stable to frequency error if we force the laser to lock to the cavity with a slight detuning from the resonance as shown by the dashed red line in Fig. 2b. We have found that offsetting the locking point from the resonance by ≈1/6 the resonance width, along with recently developed techniques to reduce the phase noise of Yb fiber combs [34], results in a stable frequency lock.

The second challenge presented by the intracavity plasma arises from the portion of the plasma density with dynamics on the femtosecond time scale, which has recently been studied in [30,31]. This effect results in a phase shift that varies over the duration of the pulse so that it is impossible to maintain constructive interference between the intracavity pulse and the incident pulse over the whole pulse duration. As a result, the intracavity pulse and corresponding spectrum become distorted. The intracavity power can clamp to a lower value than is achieved in a cavity without a plasma. While self-phase modulation resulting in blue-shifting of the spectrum has been seen in single-pass harmonic generation experiments, the effect observed in an enhancement cavity is distinct as it is magnified by the finesse of the cavity.

We make the system more robust by lowering the cavity finesse. The cavity power enhancement is proportional to

$$\frac{1}{1+\left(\frac{2\mathcal{F}}{\pi}\right)^2 \sin^2\left(\frac{\phi(t)}{2}\right)}, \tag{2}$$

#154969 - $15.00 USD Received 19 Sep 2011; revised 26 Oct 2011; accepted 27 Oct 2011; published 2 Nov 2011

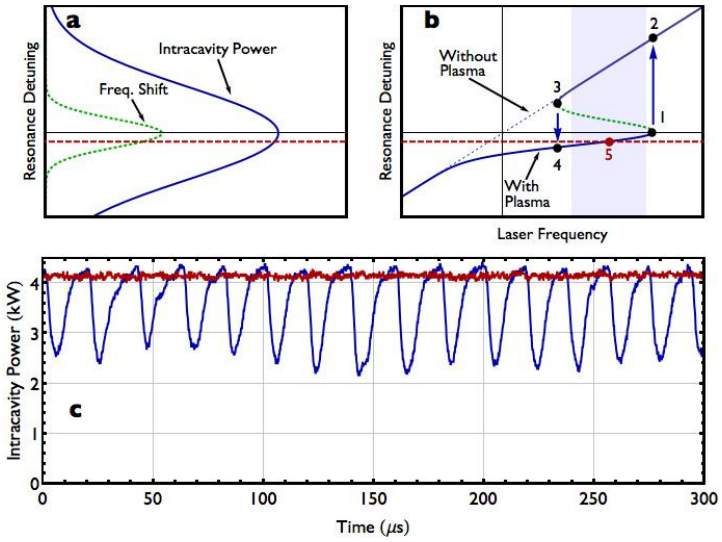

Fig. 2. a) Diagram showing both the intracavity power as a function of resonance detuning (blue curve), as well as the frequency shift in the resonance position due to plasma (dotted green curve). b) Diagram showing the detuning from the resonance as a function of the laser frequency with the shift in the resonance position shown in a) added to the otherwise linear relationship. c) Intracavity power as a function of time with an offset of the locking position from the resonance (red curve) and without an offset (blue curve). With zero offset from the resonance, the system will lock to point 1 on b). Slight laser noise at this position will cause the system to jump to point 2. The lock will then adjust the laser frequency to minimize the detuning from the resonance, moving quickly through points 2-4 on the diagram. This cycle repeats and creates characteristic oscillations as shown on the blue curve in c). By adjusting the lock so that the laser is detuned from the resonance by ≈1/6 the cavity resonance width, the system locks at point 5. This locking position is stable against frequency noise as represented by the gray box in b) and results in elimination of the oscillations as shown in the red curve in c).

where F is the cavity finesse and $\phi(t)$ is the roundtrip phase error, which we generalize to be a function of time since it varies over the duration of the pulse. Since the phase error is multiplied by the finesse, a method of mitigating the effects of a temporally varying plasma is obtained by decreasing the finesse. We accomplish this by increasing the transmission of the input coupler. This places the cavity in the overcoupled regime that results in a higher buildup for a given finesse. For instance, when the cavity loss is completely dominated by the input coupler, the buildup on resonance is given approximately by $\frac{2\mathcal{F}}{\pi}$ instead of the usual $\frac{\mathcal{F}}{\pi}$ for an impedance matched cavity (assuming perfect transverse mode matching). While lower cavity finesse significantly decreases the effects of intracavity pulse distortion, it now requires a more powerful laser to excite the enhancement cavity so that the intracavity pulse energy remains high. This challenge has been answered by recent advances in high repetition rate, high average power chirped-pulse amplified Yb fiber lasers discussed in section 2 and references [13,16,35,36]. Here, we use an enhancement cavity with a finesse of 400 to mitigate the effects of pulse and spectral distortion described above. To excite the cavity, we require a relatively large pulse energy of ~200 nJ in the external pulse train [16].

#154969 - $15.00 USD Received 19 Sep 2011; revised 26 Oct 2011; accepted 27 Oct 2011; published 2 Nov 2011

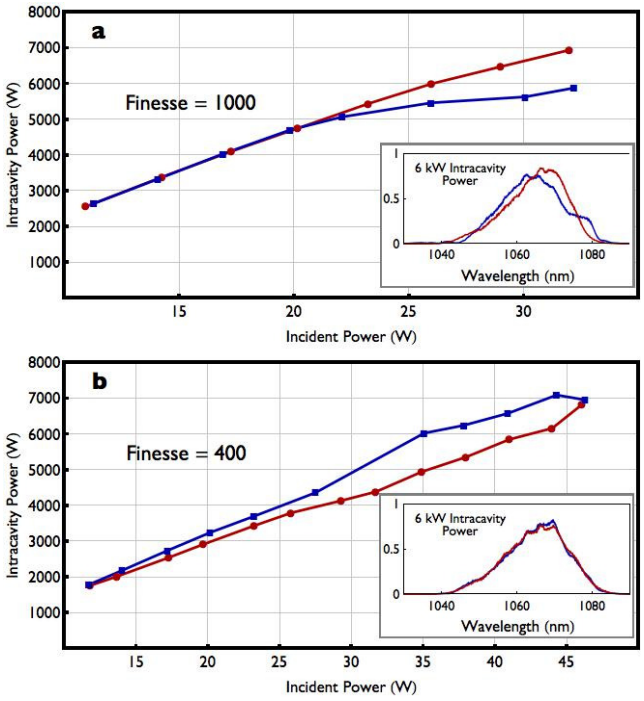

Fig. 3. a) Intracavity power as a function of incident power for a cavity with F ≈1000 for both an empty optical cavity (red circles) and an optical cavity where Xe gas was injected at the focus with a 100 μm nozzle and 1.5 atm of backing pressure (blue squares). b) Same as in a) but with F ≈400. The insets show the intracavity spectra at a representative power of 6 kW for the respective cases. Spectral distortion is clearly visible in the higher finesse cavity when intracavity plasma is present. The nozzle position with respect to the focus was identical in both cases. The mismatch in the buildup for the low finesse case is due to imperfect transverse mode matching. For the F ≈400 cavity, the power begins to clamp at 7 kW of intracavity power when Xe is used as the target gas. However, when Kr is used as the target gas (not shown) 8 kW of intracavity power is achievable.

To demonstrate the decrease in spectral distortion due to the lowering of the finesse we compare the performance of our system with two different input couplers while keeping all other parameters identical. A comparison of the intracavity spectrum and intracavity power as a function of incident power is shown in Fig. 3. Results are shown both for a target gas injected with a 100 μm diameter nozzle with a backing pressure of 1.5 atm and for no target gas. When comparing the cavities with no intracavity gas target, both cavities respond linearly with an undistorted spectrum. However, the advantage of the lower finesse cavity is clearly seen when a gas target is added at the intracavity focus. At 6 kW of average power the intracavity spectrum of the higher finesse cavity becomes distorted and the intracavity power begins to clamp while the lower finesse cavity maintains an undistorted spectrum and can still reach > 7 kW of average power.

4. Phase matching of HHG inside an enhancement cavity

It is well known that to achieve the maximum flux of XUV radiation from an HHG source the harmonic radiation must be phase-matched to the fundamental throughout the generating medium [29]. Fundamentally, these principles are no different for an intracavity source or a single-pass source. However, in practice the high-repetition rate source provides new challenges to phase-matching. Optimizing the phase-matching of an HHG source involves balancing competing phase shifts from the Gouy phase, target gas dispersion, plasma dispersion and the intensity-dependent phase of the dipole. Both the Gouy phase and the

#154969 - $15.00 USD Received 19 Sep 2011; revised 26 Oct 2011; accepted 27 Oct 2011; published 2 Nov 2011

dipole phase will vary significantly over the confocal parameter of the focused fundamental beam generating HHG, but can be made to approximately cancel at a certain focal position over a sufficiently short medium length (approximately 1/10th the confocal parameter). In intracavity HHG, the demonstrated drive pulse energies are relatively low (~100 μJ) and the pulse lengths are relatively long (~100 fs) such that tight focusing geometries are required. In our experiment the confocal parameter is ~1 mm such that we require a very short medium length of less than 100 μm. It can be challenging to produce and align such a small gas nozzle, but it is generally necessary to have such a short interaction length to generate maximum flux. Of course, it is possible to have neutral gas and plasma dispersion counteract the geometrical and dipole phase terms allowing for longer interaction lengths, but these systems must be finely tuned in a more systematic fashion.

The plasma dispersion and neutral gas dispersion produce phase shifts that are of opposite sign and can be made to cancel for a certain ionization fraction depending on the harmonic order and target gas [29]. There is once again a limiting effect when a system is pushed to ~100 MHz repetition frequency since the dispersion due to the steady state plasma (with a density ~5 times larger than the dynamic plasma density) will limit the single pass ionization to ~0.1-0.2 of what would be optimal for phase matching in a low repetition rate system. In principle, any technique that could remove residual plasma from the interaction region faster would allow for more single pass ionization with optimized phase matching and therefore could increase the XUV photon flux. Another option is to decrease the repetition rate by a factor of ~3-10 in which case the effects of the residual plasma will not offer much disadvantage (as in [12,37]). However, for XUV-DFCS, lowering the repetition rate is not ideal as the power per comb mode drops, the interpretation of spectroscopic data is more complicated (if multiple transitions are excited) and the determination of absolute comb tooth number becomes more difficult. For this reason we choose to keep our repetition frequency at 154 MHz.

5. Results and conclusion

We studied the dependence of the harmonic power as a function of intracavity power as shown in Fig. 4a. Note that there are only modest improvements in power for most harmonics as the intracavity power is increased from 5.5 to 6.5 kW. This is due in part to a decrease in phase matching as plasma density increases and also to a depletion of the on-axis neutral atom density available for HHG.

Nevertheless, we are able to generate > 200 μW and deliver ~20 μW of average power per harmonic spectrally dispersed for spectroscopy experiments [39]. Given the limitations discussed above, it seems that there are only a few avenues to increasing the harmonic power further in such a high repetition rate system. For instance, gains in harmonic power in a similar system could be achieved by increasing the focal area at the interaction region if the intracavity peak power can also be increased commensurately. Generating harmonics with a shorter-wavelength driving field can offer significant gains since the harmonic dipole scales as $\approx\lambda^{-(5-6)}$ [40]. By utilizing a fundamental wavelength of 800 nm, one could expect a gain of approximately 5 in harmonic flux for an optimized system. However, multiple-pulse optical-damage thresholds are lower [41] and the breaking of hydrocarbons is much more efficient at shorter fundamental wavelength. Therefore one may trade FEC robustness for an increase in harmonic flux.

In Fig. 4b, we compare the power of a representative harmonic (before output coupling or spectral separation) with other high performance HHG systems [12,29,37,42–45]. Our system compares favorably with the system very recently reported in [12] when one considers that the latter system employs an 800 nm driving field. The repetition frequency for that system is 50 MHz so that the power per comb mode for that system and our system is roughly the same. Additionally, our system is, so far, the only high-repetition rate system capable of delivering a large fraction of our spectrally separated harmonic power to a subsequent spectroscopy

#154969 - $15.00 USD Received 19 Sep 2011; revised 26 Oct 2011; accepted 27 Oct 2011; published 2 Nov 2011

experiment. It is interesting to note that our source, along with that demonstrated in [12], is now within an order of magnitude of the spectral brightness of an Advanced Light Source undulator operating at similar wavelength [46].

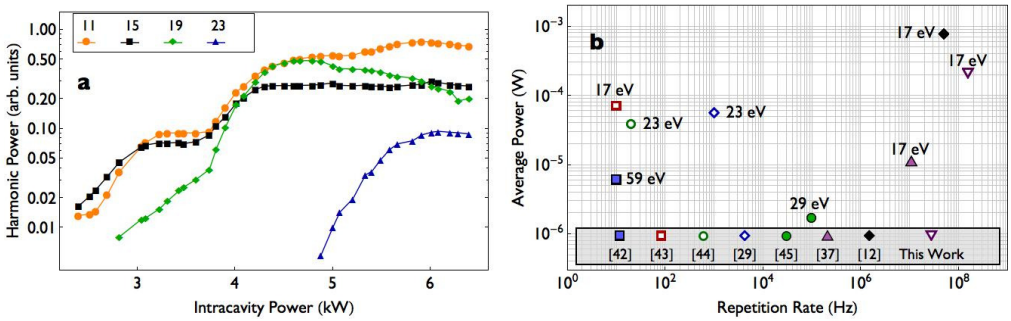

Fig. 4. a) Harmonic power plotted as a function of intracavity power for all harmonics showing a marginal increase in harmonic power for intracavity powers between 5.5 and 6.5 kW. The oscillations visible for some harmonics are due to quantum path interference [38] b) Comparison of the generated power of high performance HHG systems for representative harmonics. Reference [12] and [37] are also intracavity harmonic systems operating at ~800 nm but with collinear output coupling that requires additional spectral filtering before spectroscopic experiments. As described in the text, the shorter fundamental wavelength will tend to produce higher flux. Our system in the only one in the figure not utilizing Ti:Sapp and operating at fundamental wavelength around 1 μm.

In conclusion, we present an intracavity HHG system which overcomes many technical limits and is capable of delivering a high average flux of harmonic photons to direct frequency comb spectroscopy experiments in the XUV. Using this system we have recently been able to perform spectroscopy on a skimmed atomic beam of neutral argon atoms and have demonstrated the first DFCS at XUV wavelengths [39].

Acknowledgments

This research is funded by DARPA, AFOSR, NIST, and NSF. A. Cingöz and T. K. Allison are National Research Council postdoctoral fellows. A. Ruehl acknowledges funding from the A. von Humboldt Foundation (Germany). We thank P. A. Hermann and M. Ahmed for useful discussions.

#154969 - $15.00 USD Received 19 Sep 2011; revised 26 Oct 2011; accepted 27 Oct 2011; published 2 Nov 2011